

New Phytologist
Supporting Information

STALK CELL POLAR ION TRANSPORT PROVIDE FOR BLADDER-BASED SALINITY TOLERANCE IN
CHENOPODIUM QUINOA

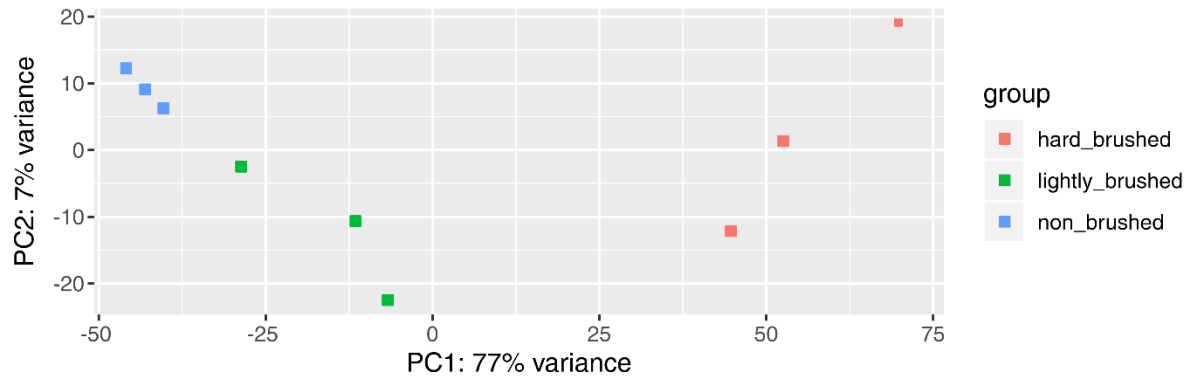
Nadia Bazihizina, Jennifer Böhm, Maxim Messerer, Christian Stigloher, Heike M. Müller, Tracey Ann Cuin, Tobias Maierhofer, Joan Cabot, Klaus F.X. Mayer, Christian Fella, Shouguang Huang, Khaled A.S. Al-Rasheid, Saleh Alquraishi, Michael Breadmore, Stefano Mancuso, Sergey Shabala, Peter Ache, Heng Zhang, Jian-Kang Zhu, Rainer Hedrich, Sönke Scherzer

article acceptance date: 12 April 2022.

Supporting Figures

Figure S1

A



B

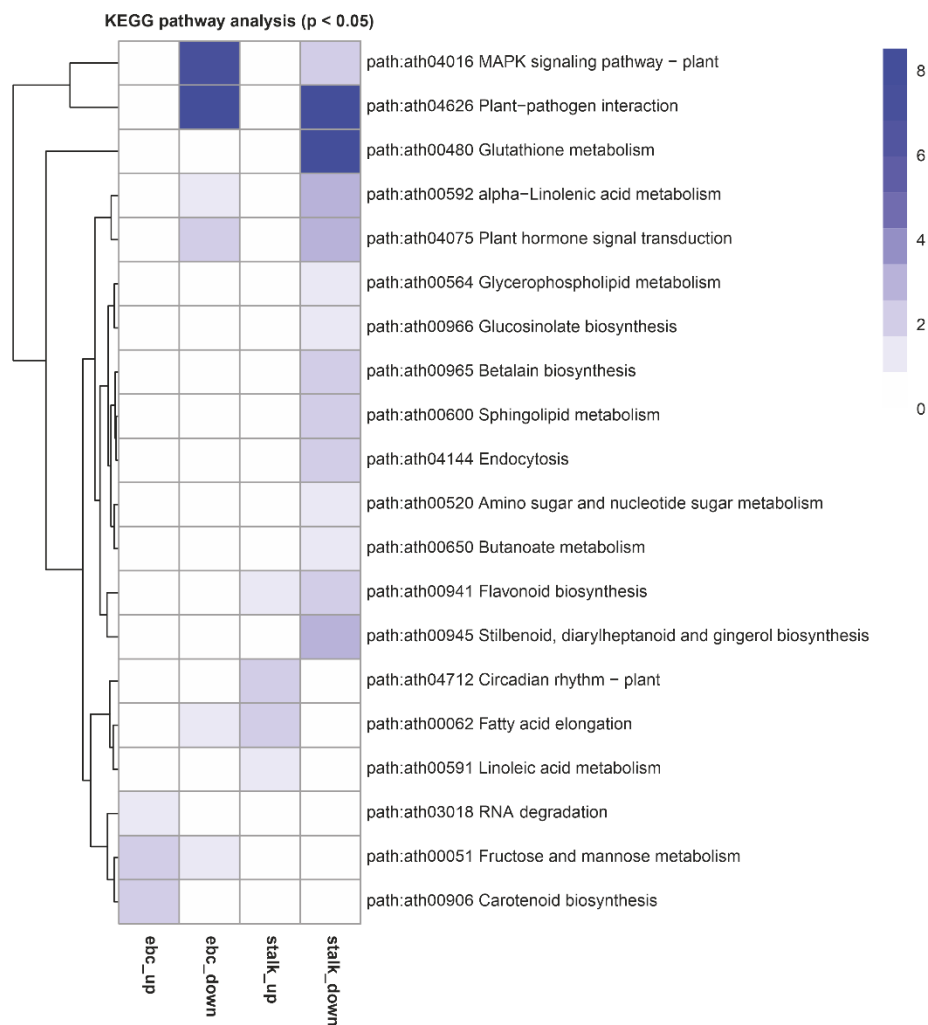
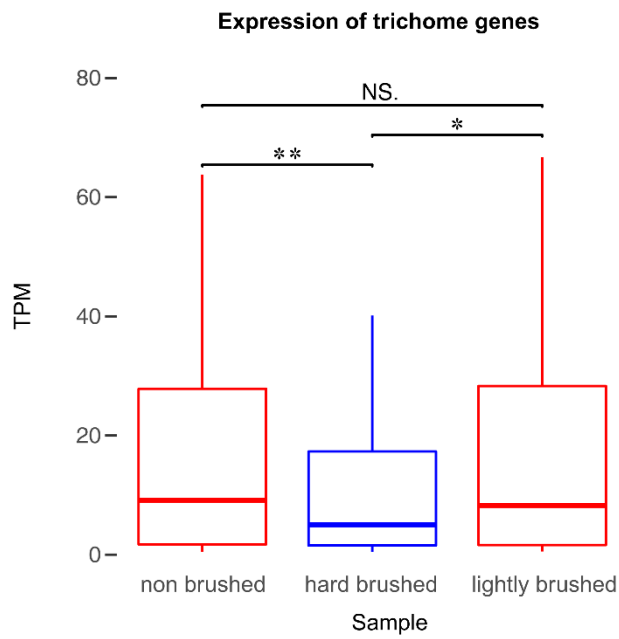


Figure S1: Bioinformatical analysis of stalk cells.

(A) Principal component analysis (PCA) of generated *quinoa* preparations. (B) Enrichment of KEGG (Kyoto Encyclopaedia of Genes and Genomes) pathways for up- and down-regulated SC and EBC DEGs. Colouring according to $-\log_{10}(\text{p-value})$. (*Related to Figure S2 and to supporting information Methods*)

Figure S2

A



B

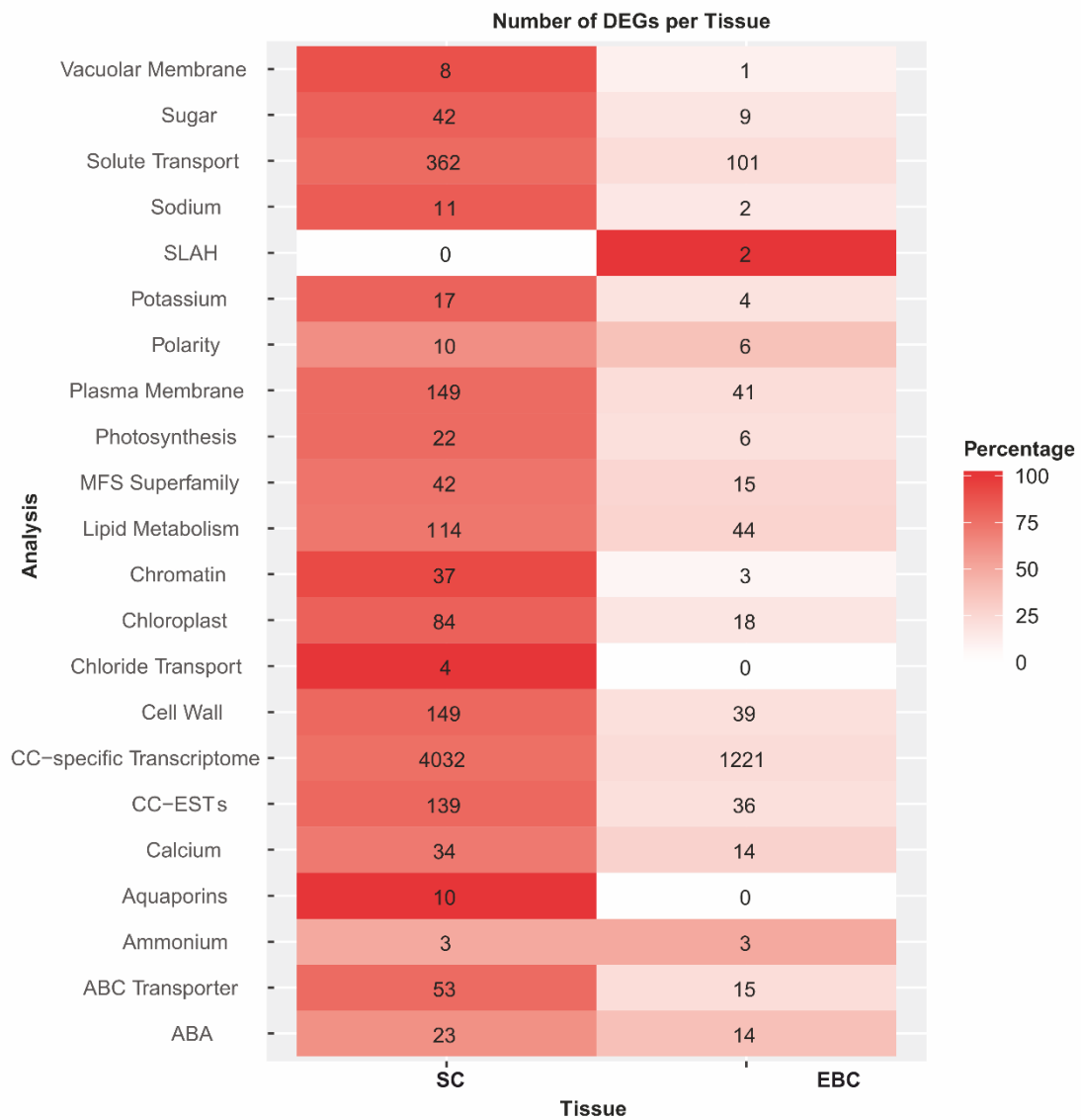


Figure S2: The number of DEGs is far higher in SCs compared to EBCs.

(A) Comparison of TPM (transcripts per million) expression values of trichome specific genes for non-, lightly- and hard-brushed samples. Expression of these genes was significantly reduced in the hard-brushed sample which does not contains stalk cells (SCs) and thus pointing to a high cell purity of the samples (asterix indicate * $p < 0.05$ and ** $p < 0.01$ by one-way ANOVA; NS not significant). (B) Heatmap showing the number of differentially expressed genes (DEGs) for SCs and EBCs. Analysis reflects the assigned genes mentioned in the manuscript. Colouring is according to the percentage of summed SC and EBC DEGs. (See also *Figure S1, S6-8 and Table S1*)

Figure S3

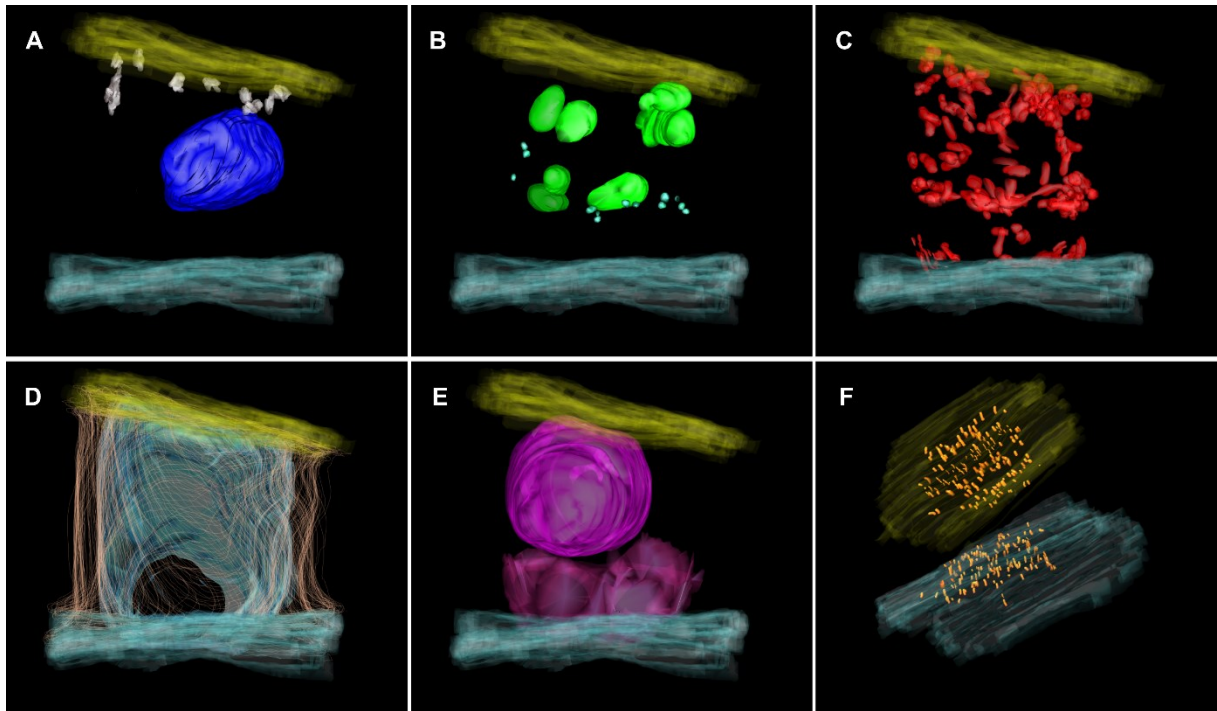


Figure S3: Ultrastructure of stalk cells.

(A-E) The 3D reconstruction of the SC ultrastructure illustrates the basal (epidermal) cell wall (blue), apical (bladder-facing) cell wall (yellow), and single organelles within the transfer cell. (A) nucleus (dark blue), Golgi complexes (grey); (B) chloroplast (green), multivesicular-bodies (turquoise); (C) mitochondria (red); (D) lateral (outer) cell wall (fine lines), membrane (light blue); (E) fragmented vacuoles (purple). To illustrate locations of plasmodesmata (golden) the model was tilted (F).
(Related to Figure 1)

Figure S4

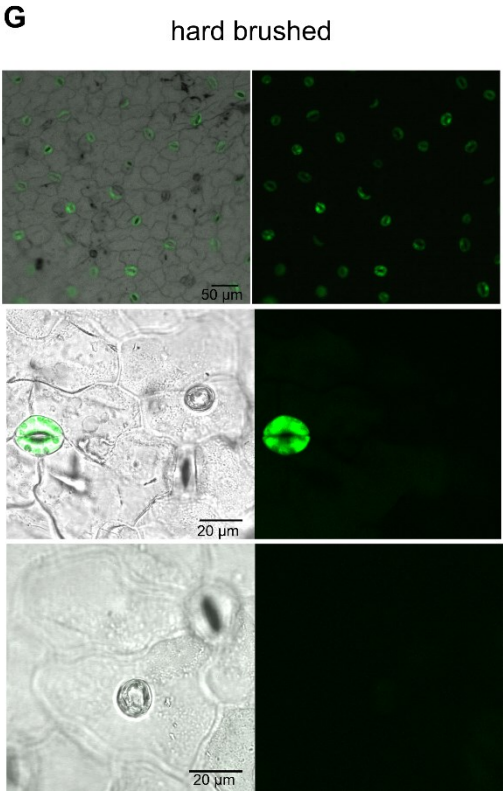
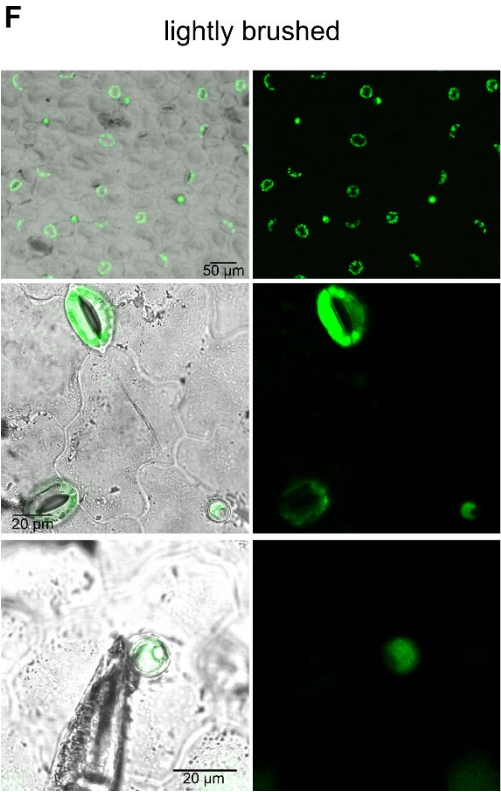
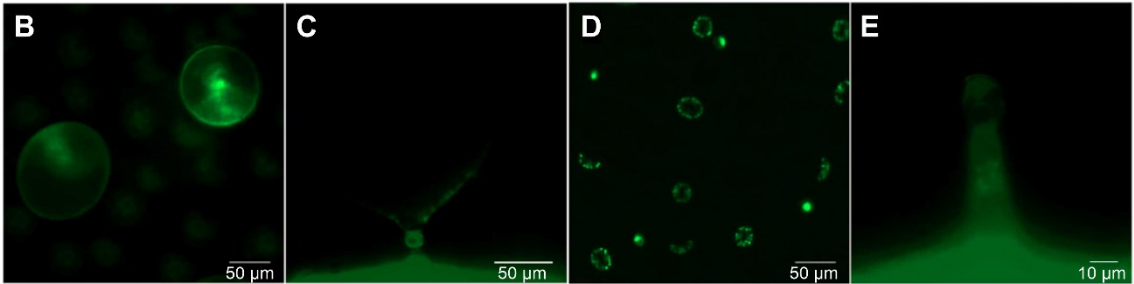
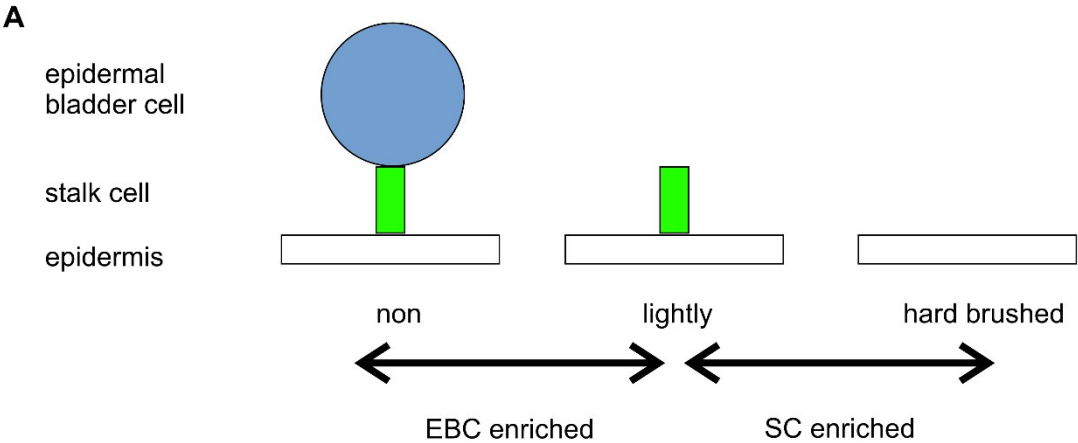


Figure S4: Stalk cell isolation procedure and vitality check of the de-bladdered stalk cell for bioinformatical analysis.

(A) Model of EBC (blue), SC (green), and EC (white) among the 3 treatments (non-, light- and hard-brushed). The indicated differential expression analysis (arrows) indicates EBG-enriched and SC-enriched genes. Apical (B) and lateral (C) view of an intact epidermal bladder cell and stalk cell complex stained with fluorescein diacetate. Apical (D) and lateral (E) view of intact de-bladdered stalk cells stained with fluorescein diacetate. Apical view of (F) lightly brushed epidermis after fluorescein diacetate staining showing both living guard cells and SCs. After hard brushing (G), only guard cells are alive in the same treatment. (*Related to Figure S2*)

Figure S5

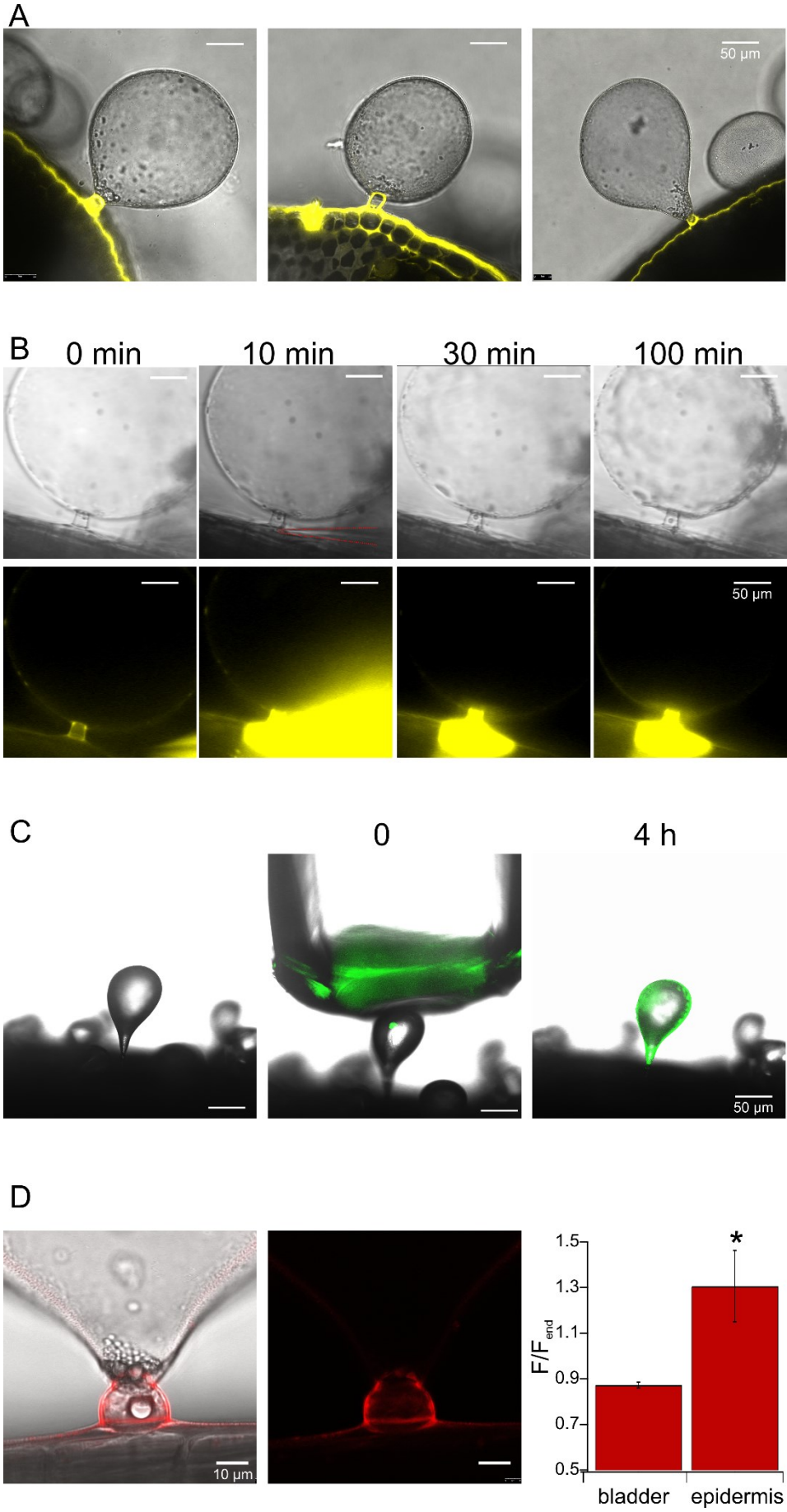


Figure S5: Staining experiments show no symplastic connection between SC and EBC and a trans SC voltage gradient.

(A) Quinoa leaves were fed for 36 hours with 1 mM Lucifer yellow dissolved in deionised water via the petiole. In 3 representative images, staining of petiole localized SCs but not the EBCs is evident. (B) Lucifer yellow was iontophoretically loaded into the EC that is adjacent to a SC, with a single barrel microelectrode, as indicated in the brightfield image at 10 min. Note that the dye rapidly travelled from the epidermal cell to the stalk cell, whereas it failed to go into the bladder cell. A total of 4 experiments were conducted, which showed very similar results. (C) Staining of an EBC (left) with 5 μ M membrane-permeable CFDA ((5-(and-6)-carboxyfluorescein diacetate)) diffused through a capillary (middle). Once inside cells, CFDA is hydrolyzed by intracellular esterases to 5-carboxyfluorescein and can no longer diffuse freely across membranes. Without a symplastic connection between EBC and SC, CFDA does not enter the SC even after 4 hours (right). (D) Staining of intact SCs with ANNINE-6plus (left overlay; middle emission spectrum). After washing out, the fluorescence intensity (F) of the SC plasma membrane was determined on the side facing the bladder and the side facing the epidermis. Subsequently, the samples were treated with 1% saponin. After 5 min both intensities were determined again (F_{end}). Normalisation (F/F_{end}) (right) revealed a higher F/F_{end} ratio at the epidermal side, which corresponds to a hyperpolarised potential (mean \pm SE; n = 3; student's t-test *, p < 0.05).

Figure S6

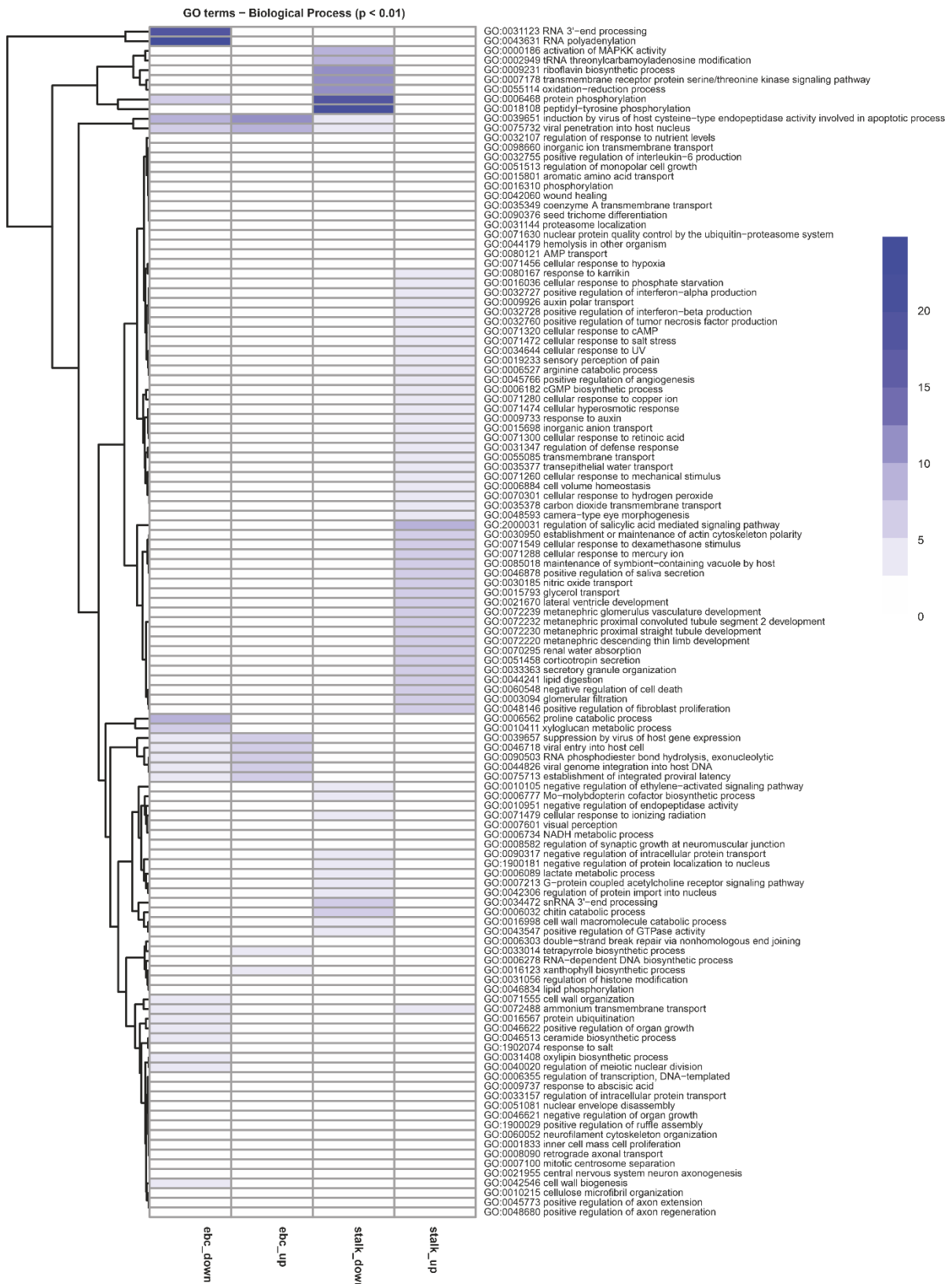


Figure S6: GO term – Biological Process.

GO term enrichment for Biological Process (BP) for up- and down-regulated SC and EBC DEGs. Colouring according to $-\log_{10}(p\text{-value})$. (Related to Figure 2)

Figure S7

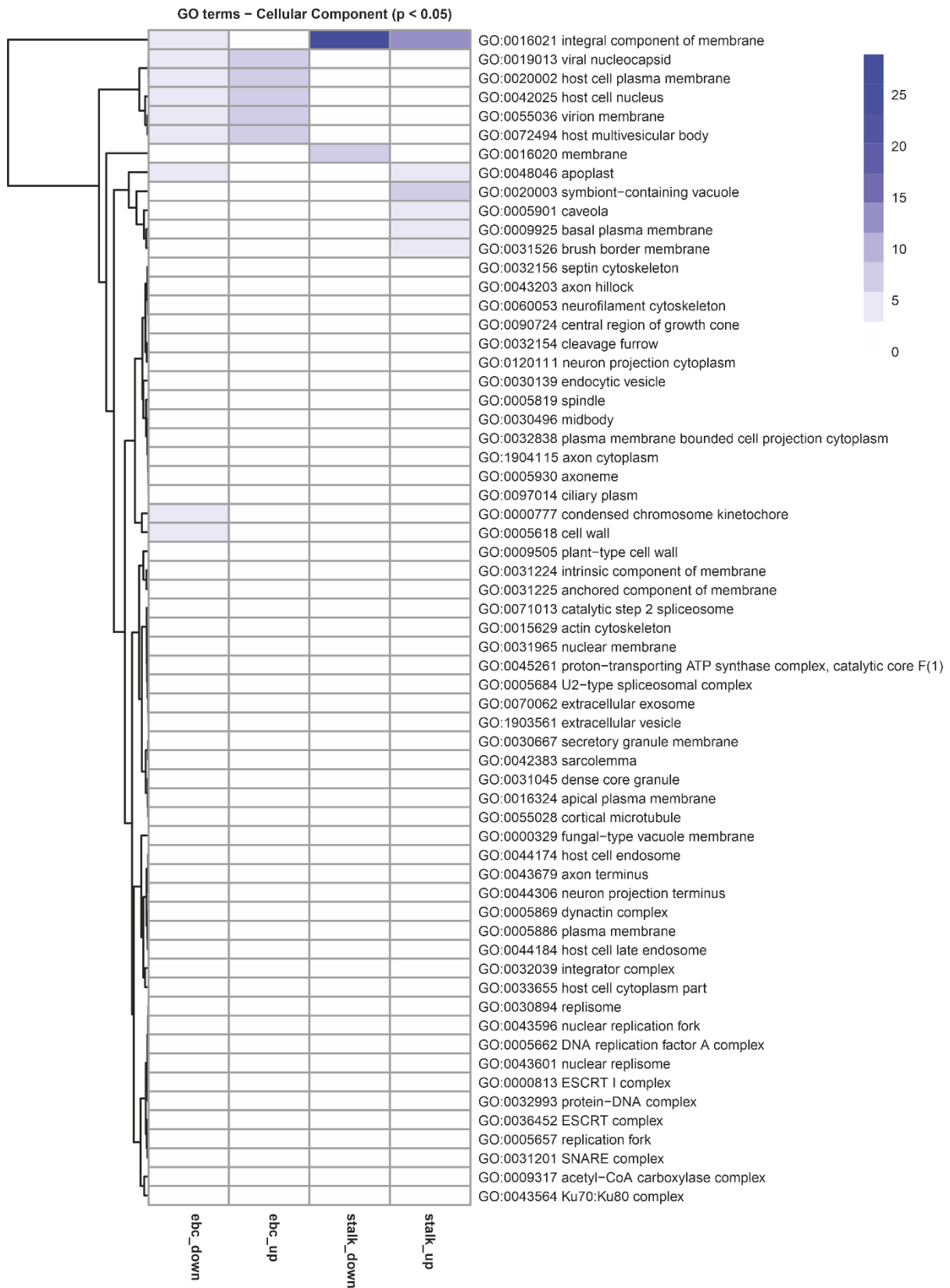


Figure S7: GO term – Cellular Component.

GO term enrichment for Cellular Component (CC) for up- and down-regulated SC and EBC DEGs.

Colouring according to $-\log_{10}(p\text{-value})$. (Related to Figure 2)

Figure S8

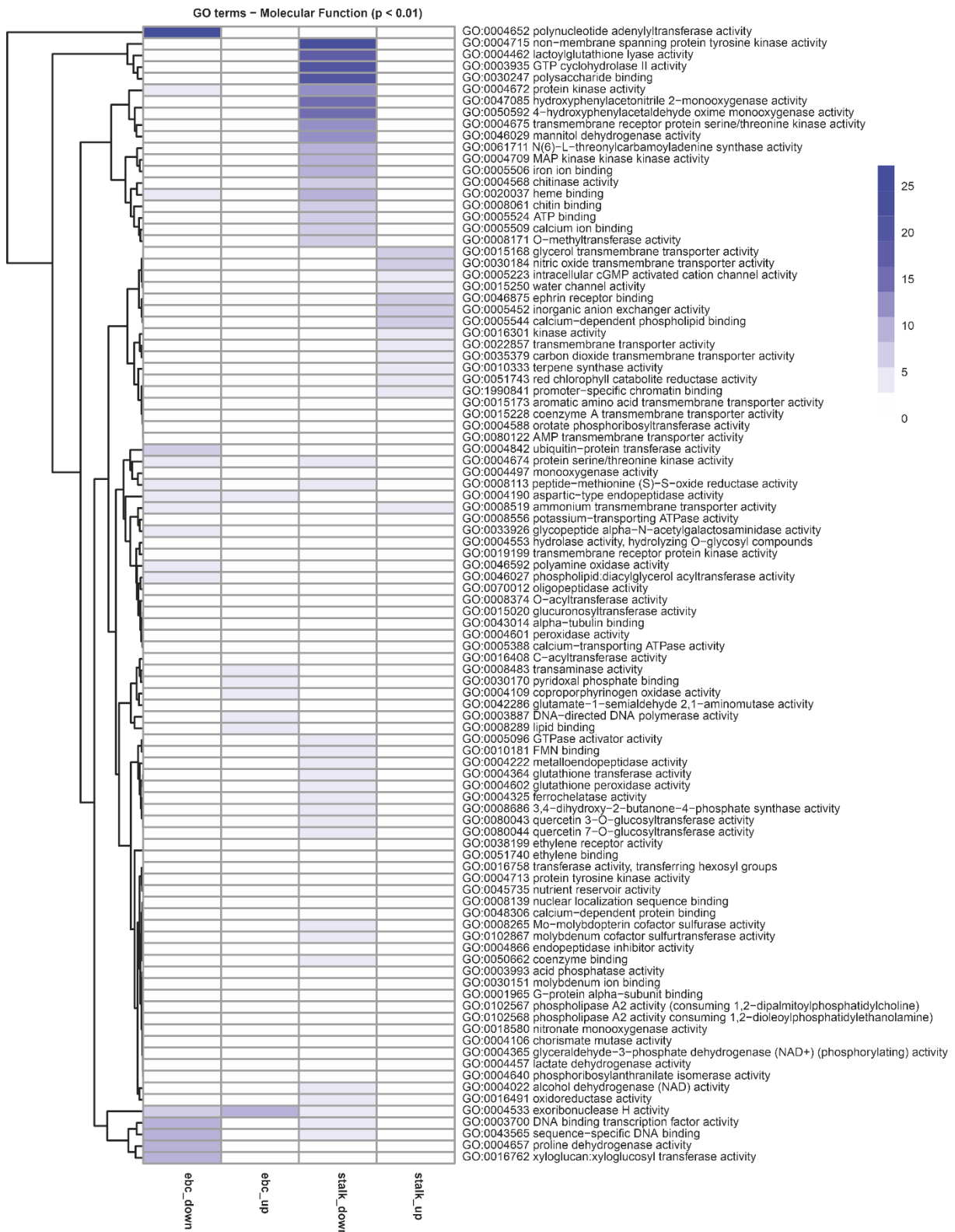


Figure S8: GO term – Molecular Function.

GO term enrichment for Molecular Function (MF) for up- and down-regulated SC and EBC DEGs.

Colouring according to $-\log_{10}(p\text{-value})$. (Related to Figure 2)

Figure S9

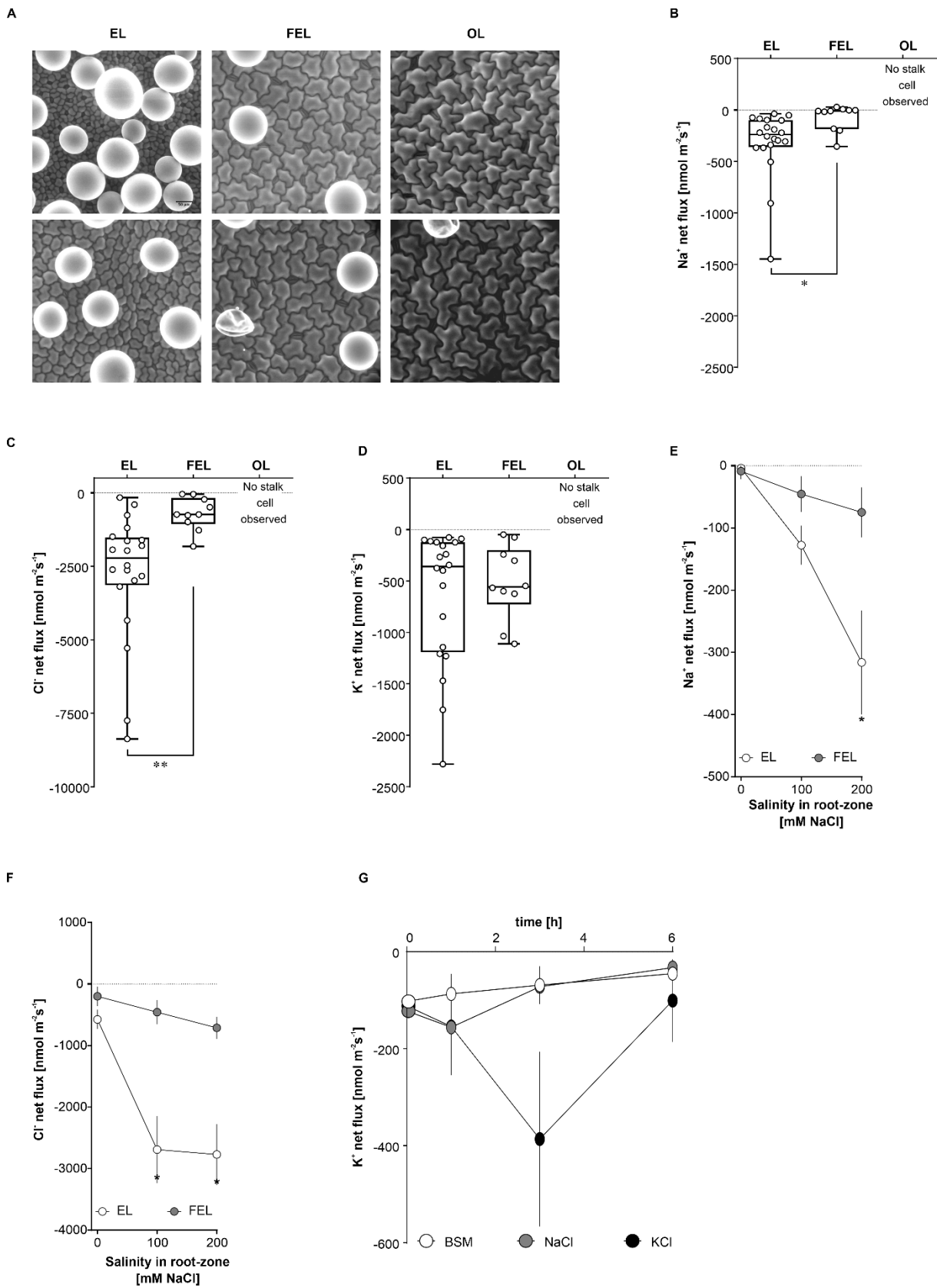


Figure S9: Ion fluxes in stalk cells on petioles of quinoa leaves (accession Q20).

(A) Scanning electron microscope images of the leaf surface showing bladder density at each leaf age. The plots summarise Na^+ (B), Cl^- (C) and K^+ (D) fluxes measured in the apical poles of isolated stalk cells on petioles from leaves of different ages in 5 week old plants. The box and whisker plots denote the minimum, 25th percentile, median, 75th percentile and maximum values. Net Na^+ (E) and Cl^- (F) fluxes measured in the apical poles of isolated stalk cells in young expanding leaves (EL) and fully expanded leaves (FEL) under control and saline (200 mM NaCl) conditions. In old leaves (OL) no viable stalk cells were observed. Values are mean \pm SEM, $n = 5$ (with each replicate being the average of two measurements from separate SCs in EL and one measurement in FEL). (G) Stalk cell transcellular K^+ flux dynamics measurements of the apical pole of de-bladdered stalk cells without salt application (white circles), NaCl (grey circles), or KCl-feeding via the xylem. ($n \geq 5$ experiments, mean \pm SEM). (*Related to Figure 4*)

Figure S10

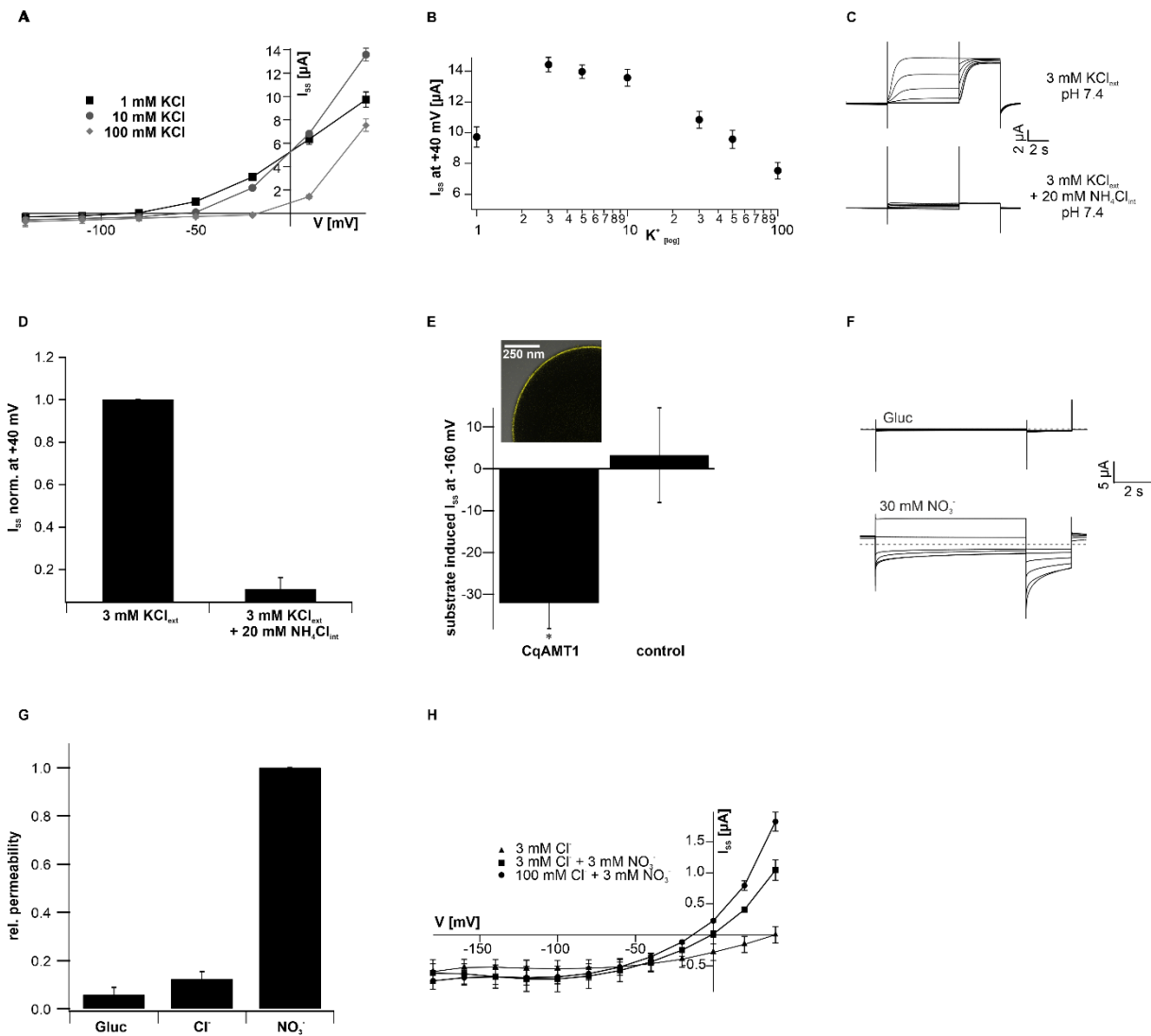


Figure S10: Electrophysiological characteristic of stalk cell expressed transport proteins.

(A) Steady state currents (I_{ss}) over a voltage range of -140 to +40 mV of CqSKOR-expressing oocytes are shown. Only outward rectifying currents (positive) were observed in the bath medium with the indicated K^+ concentration at pH 7.4. With a reduction in the external K^+ concentration, the activation threshold shifted to a more negative membrane potential. ($n = 5$ experiments, mean \pm SD) (B) CqSKOR mediated I_{ss} at +40 mV were plotted against the logarithmic scale of the applied K^+ concentration, revealing a current optimum between 3 and 10 mM external KCl. ($n = 5$ experiments, mean \pm SD) (C-D) CqSKOR-expressing oocytes were perfused with 3 mM KCl and either injected with water (C, upper panel) or 20 mM NH_4Cl (C, lower panel) during TEVC measurements. By injecting NH_4Cl , the CqSKOR mediated outward currents (positive) declined by nearly 90% and the statistical analysis of the normalised efflux I_{ss} at +40 mV is seen in (D). ($n = 9$ experiments, mean \pm SD) (E)

Localisation studies of YFP::CqAMT1 fusion constructs in *X. laevis* oocytes (inset) displayed the YFP signal on the surface of the plasma membrane. A representative image is shown. The substrate induced NH_4 -influx I_{ss} of CqAMT1-expressing oocytes clamped at -160 mV and perfused with 2 mM NH_4Cl are shown compared to control cells. ($n \geq 6$ experiments, mean \pm SEM; significant differences using two-sided Student's t-test, $*P < 0.02$). (F) Whole oocyte current traces of oocytes expressing CqSLAH3 in either gluconate or nitrate (30 mM) based standard buffers. Representative currents are shown and dotted line represents 0 μA (please note that negative currents represent anion efflux). (G) Relative permeability of CqSLAH3 expressed in *Xenopus* oocytes for physiological relevant anions chloride (Cl^-) and nitrate (NO_3^-) compared to non-permeable gluconate (Gluc). Permeability for nitrate was set to 1. ($n = 4$ experiments, mean \pm SD) (H) Steady-state currents (I_{ss}) of CqSLAH3 expressing oocytes plotted against the applied voltage. Currents were recorded in standard buffers containing different chloride/nitrate ratios, as indicated in the figure ($n = 4$ experiments, mean \pm SD). (Related to Figure 5)

supporting Tables

Table S1: Bioinformatical analysis of the stalk cell transcriptome.

(Related to Figure S2)

supporting Video

Video 1: Combination of X-ray imaging of resin embedded sample to efficiently target stalk cell of interest and serial section transmission electron microscopy (TEM) imaging for analysis of the ultrastructure at high resolution and 3D.

The video starts with a lower magnification nanoCT tomogram overview of a high pressure, freeze substituted and resin embedded sample block in order to identify a stalk cell of interest. The coordinates of the identified cell in the nanoCT scan can then be used to readily target the object of interest for ultrathin sectioning. At the TEM, the serial sections can be imaged to readily find the stalk cell of interest. Ultrastructural details can be imaged and analysed as shown by a high-resolution image of a chloroplast. Furthermore, after acquiring the same cell in the serial sections, they can be aligned and the cell can be explored in 3D. (Related to Figure 1)